ANALYSIS OF THE DYNAMIC STRESSES IN THE CATENARY PROFILE OVERLAND CONVEYOR NUMBER B18 AT GOEDEHOOP COLLIERY.

Hector Neville Dreyer.

A project report submitted to the Faculty of Engineering, University of the Witwatersrand, Johannesburg, in partial fulfilment of the requirement for the degree of Master of Science in Engineering.

JOHANNESBURG, 1988

I DECLARE THAT THIS PROJECT REPORT IS MY OWN, UNAIDED WORK. IT IS BEING SUBMITTED FOR THE DEGREE OF MASTER OF SCIENCE IN ENGINEERING AT THE UNIVERSITY OF THE WITWATERSRAND, JOHANNESBURG. IT HAS NOT BEEN SUBMITTED BEFORE FOR ANY DEGREE OR EXAMINATION IN ANY OTHER UNIVERSITY.

....

H.N. DREYER.

......31 st...... DAY OF ......August......198 8

A B S T R A C T

High oscillating tensions during stopping caused severe damage to the take-up structure of the B18 conveyor at Goedehoop Colliery. Shut down behaviour of a conveyor belt cannot be studied without also referring to the subsequent re-starting behaviour.

Every conveyor installation is unique. It is therefore necessary to study the behaviour of each installation separately in order to optimise the adjustments affecting the performance of the system-

The project report describes the field tests performed to measure the stresses at various locations along the length of this long o Land conveyor. Test results are discussed in detail.

Ways of reducing the magnitudes of dynamic stresses and preventing their occurrence in B18 conveyor are suggested to improve the life and availability of the conveyor.

Controlled starting has been successful on this installation as in others but during stopping when all power is lost the most effective method of arresting dynamic stresses was found to be the controlled release of "stored" belt tension.

TO MARIANNE AND OUR BOYS

ACKNOWLEDGEMENTS.

Thank you Brian Smith, Jenny Rudd and Alf van Dijk for your able support. Also to the management of the Coal Division of Anglo American Corporation of South Africa for permission to publish this report and to the Management of Goedehoop Colliery for assistance provided during the project investigation. A special word of thanks to Danny Cipolat, my project supervisor.

C O N T E N T S

ANNEXURES

LIST OF FIGURES

FIGURE		PAGE

FIGURE		PAGE

FIGURE		PAGE

LIST OF TABLES

CHAPTER 1

1. OVERVIEW

1.1 STATEMENT OF THE PROBLEM.

Recent years have seen the development of longer and higher capacity belt conveyor systems. Part of this development was the introduction of high speed conveyor belts. This had the desired effect of reducing capital cost of such systems since relatively narrow belts were now able to convey large quantities of material.

Unfortunately catastrophic failures started occurring as well. New problems associated mainly with long and/or high speed conveyor belts were discovered. These mostly related to the presence of dynamic stresses in the belting.

During the acceleration and deceleration phases of the belt motion (i.e. during starting and shutdown) stress waves develop. These stresses were never considered in conventional design calculations and were therefore never predicted. Consequently structural designers never took this into consideration when designing conveyor structures. Conventional design considered the conveyor belt as a rigid body. This approach assumed that the entire length of belt started moving as the drive pulley started moving.

This assumption is obviously not true, but it simplified design calculations and always seemed to be effective for the conventionally short, low speed conveyor systems.

1.2 CASE STUDY.

The B18 overland conveyor at Goedehoop Colliery was designed using conventional methods. At 1 700 metres between belt centres it is certainly not a long conveyor by modern standards. It would rather be classified as a medium length conveyor system. The designed belt speed of 3,85 metres/second also puts it into the medium range of belt speeds.

The conveyor runs through a valley as shown in figure 1.1. The catenary shape introduced major dynamic stress waves in the belting during shut down.

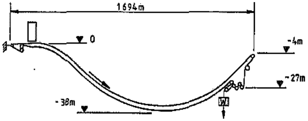

Figure 1.1 Cross section of B18 conveyor

Shortly after commissioning the system in October 1985 the conveyor was tripped under overloaded conditions. During this emergency shut down the stress shock waves set up in the belt reacted at the gravity take-up system C shown in figure 2. The sudden increase in stress at the take-up caused the take-up pulley, E to shoot forward. This in turn caused the take-up weights, D to shoot up through the top of the take-up tower when the rope connecting the take-up pulley and gravity weight snapped. The 13 tons take-up weight then dropped through five metres to destroy the take-up tower structure - and itself!

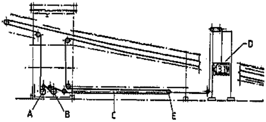

Figure 1.2 B18 conveyor drive and gravity take-up arrangement.

A: Secondary drive pulley

B: Primary drive pulley

C: Gravity take-up system

D: Take-up weights

E: Take-up pulley

Emergency repairs were done and the system was recommissioned with a motorised winch take-up and limited to operate at a maximum of 800 tons per hour. The required capacity was 1 000 tons per hour and the designed capacity 1 200 tons per hour.

1.3 AIM OF THIS STUDY.

The dynamic shock wave problem has only raised its head in the last decade. In this period relatively few systems experienced shock wave problems to the extent that drastic steps were necessary to overcome them. It is therefore understandable that no set behaviour pattern of conveyor shock waves has been established to date. At least two mathematical models have been developed to describe conveyor dynamic stress behaviour (Morrison, 1985 and Nordell, 1984) but none of these have been calibrated to cater for a variety of conditions pertaining to real problem installations.

The purpose of this study is to determine from an analysis of test measurements taken over a period the magnitude and motion of the dynamic stresses present in the B18 conveyor belting during the starting and shut down cycles of the system. The study will also research the origin of these stresses and analyse the factors which influence the dynamic stresses.

1.4 FORM OF REPORT

The following sections of this report contain a summary of existing literature on this subject followed by a description of the field test programme conducted during the study of stresses in B18 conveyor.

Observations and results are discussed to highlight the source of the dynamic stress waves detected in the B18 conveyor and the behaviour of the conveyor during shut down and acceleration cycles with specific reference to dynamic stress waves and factors influencing it.

Finally a conclusion is drawn followed by recommendations to minimise dynamic stresses in B18 conveyor and proposals for further research in this field are discussed.

CHAPTER 2

LITERATURE REVIEW.

Since the early 1980's several papers have been published on dynamic stresses in conveyor belts. Research has taken place in Australia, the U.S.A. and Germany.

The subject of dynamic stresses in belt conveyors was raised at virtually every belt conveying conference held in the 1980's.

One of the earliest papers on this subject was written by Harrison and Roberts (1983). They recognised the need to reduce belting cost. by reducing belt stresses. They noted the high dynamic tensions in belting during stopping and starting cycles. Their analysis indicated that shock waves resulted from discontinuities in the drive system during acceleration such as the switching in of secondary drives and the sudden removal of drive power when shutting a conveyor system down.

Figure. 2.1 shows the ideal acceleration S curve, as suggested by Harrison & Roberts (1983). The deceleration cycle should be a mirror image of this curve.

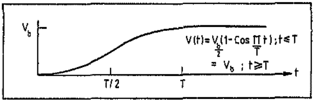

Figure 2.1 Ideal belt velocity characteristic to minimise transient tensions at start and stop (Harrison and Roberts, 1983).

This paper also illustrates the detrimental effect of applying severe braking torque to a downhill regenerative conveyor belt namely severe stress fluctuations in the belting.

Harrison published another paper on the subject (1986). He reported on dynamic stress front velocities in steel chord belting. His tests were conducted in a laboratory. He showed that belt tension is proportional to stress front velocity and that stress front velocity is approximately equal to the speed of sound in steel chord belting.

Factors damping stress fronts (i.e. causing retardation) were found to be:

a. Idler contact - which is related to belt tension and number of idlers.

b. Belt loading.

Harrison also published a paper describing methods of reducing dynamic loads in conveyor belting (1985). He showed that dynamic stress is proportional to instantaneous belt velocity.

He also listed possible sources from which dynamic stresses can be generated during conveyor starting and shut down cycles. These are:

a. Large starting torque.

b. Long take-up loops.

c. Incorrect belt pre-tension before start-up.

d. Rapid belt deceleraton.

Harrisons' account of events during a starting cycle is as follows:

"During the start-up of gravity take-up systems, the gravity take-up moves down as the drive drum rotates. If the return belt tension is less than the mass take-up force, the return belt does not move until the stress in the carry side has propagated around the whole belt. At this point, the take-up mass is required to move up as the return belt surges to a substantial proportion of the final belt speed.

The stress in the belt and structure of this type of design may be ten times the static stress. A long take-up loop in this situation causes instabilities in the belt at the tail due to the need to accommodate the extra belting as the return belt surges around the tail pulley and catches up with the carry-side belt. A small differential velocity causes severe belt sag and material spillage as the belt is pulled tight by continuing drive tension. This effect also occurs at conveyor shut down."

Harrison proposed several solutions to the problem:

a. The use of wound rotor motors with stepped rotor resistance control to apply and remove driving torque in acceptably small increments.

b. The use of short take-up loops.

c. Using optimum pre-tensioning of the belt before applying starting torque.

d. The use of winch controlled take-up rather than gravity take-up to provide high enough starting pre-tension and a reduced running tension during steady state conditions.

e. The use of a hydraulic buffer at the head drive gravity take-up trolley to provide additional belt tension as the forward running take-up trolley is checked by the hydraulic buffer.

Harrison warned about the danger associated with the use of winch controlled gravity take-up systems.

a. Winch motion must be synchronised with belt motion to prevent the winch winding in at the same time as the arrival of a dynamic shockwave at the take-up pulley. This would result in unacceptably high instantaneous stresses in the belting which in turn can lead to belt splice failure.
b. Winch reaction time is slow.

He concludes that "unless the dynamic behaviour of the belt is exactly known for all conditions of load, it is very dangerous to expect the winch to track dynamic tensions automatically during stopping in particular, and to maintain uniform belt and structure load. The phase between the winch action and the belt motion is critical if higher stresses are not to be produced into the structure".

Nordell (1984), published a paper on the subject in which he presented an introduction to the modern analysis techniques used in determining the magnitude of the dynamic transient forces propagated in a conveyor belt during its starting and stopping phases.

He defined Rheology as "the science dealing with the deformation and flow of matter" and proceeded to describe a finite element rheological model approach to determine the true nature of the belts physical behaviour. The model describing the belts dynamic response is represented by figure 2.2.

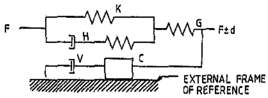

Figure 2.2 Five element composite model (Nordell, 1/84).

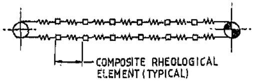

Figure 2.3 Lump mass spring-dampened finite element model (Nordell, 1984).

Referring to figure 2.2

K: Elastic modulus of the belt material as in a spring obeying Hookes' law.

H: Rolling friction or indentation loss of the belt in contact with belt rollers. It is represented by a combination of a dash pot and a spring.

G: Belt sag between idlers.

V: Conveyor drive losses i.e. the rotating elements.

C: Transitional static to dynamic friction analagous to a sliding block on a dry surface.

Dynamic simulation of the complete conveyor is accomplished by dividing the belt into a specified series of finite elements each having a lumped mass and an individual rheological spring response structure shown in figure 2.3 above.

The general equation of motion, which describes the transient force-displacement relationship, is given in the form:

$$F(t) = M\ddot{x} + K_1 x + V\dot{x} + H(\dot{x},x) + C(x,F(t)) + G(x)$$

where, $F_{(t)}$ = Force applied on an element at time t.

M = Mass matrix

K_1 = Elastic spring constant matrix of belt main tensile member

V = Viscosity matrix of the fluid element

H = Hysteresis internal damping of the belt

C = Coulomb drag matrix

G = Geometric stiffness matrix of axial motion

x = Displacement axially along belt line

$\dot{x}$ = Velocity axially along belt line

$\ddot{x}$ = Acceleration axially along belt line

t = Time

Nordell (1984) published results of some case studies to illustrate some of the problems encountered during starting and stopping of a conveyor system. He concluded that stopping of a large high modulus belt is potentially more damaging, is less controllable, and is more difficult to assess than the action of starting. The belts internally stored strain energy reacts with a higher specific impulse than can be generated by the drive system.

In 1987 Nordell presented a paper giving details of further tests on starting and stopping control to illustrate common problems in belt conveyor design.

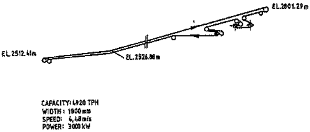

Figure 2.4 Belt profile - study no. 1. (Nordell, 1987)

His observations were:

(i) Total driving power drops off in less that one second.

(ii) Drive pulley retards 30% in one second.

(iii) Belt return strand tensile stress wave velocity is 1740m/s.

(iv) Peak stress wave value at the fixed take-up is 925kN after 3,5 seconds (operating tension at this point is 300kN).

(v) Peak stress value at the tail is 525 kN after 1,5 seconds (nominal operating tension at this point is 45kN).

(vi) Loaded side stress wave velocity is 1 390 m/s.

(vii) Violent belt whip was apparent in the concave curve zone corresponding to violent belt velocity variations at this point.

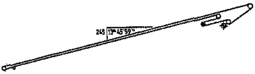

Figure 2.5 Belt profile - study no. 2. (Nordell, 1987)

Nordells observations were:

(i) A sudden shock wave hit the gravity take-up after 7,5 seconds.

(ii) The tail pulley was subjected to a shock wave at t = 7 seconds after having been at zero tension between t = 1 and t = 6 seconds.

(iii) The belt motion at the tail reversed up to 66 m/s and at the take-up 150 m/s.

(iv) The head pulley stopped in 2 seconds while the rest of the system took 14 seconds to settle.

He concluded that the studying of many conveyors which exhibit bizarre and sometimes violent behaviour expands the designers understanding to allow for better generalisation on all design aspects.

Further case studies were discussed in a paper by Surtees (1986). The paper described case studies of a conveyor suspected of having high transient stresses. Results of field measurements were analysed with simple correlation to existing mathematical models.

The paper concentrated on starting of conveyors and referred briefly to stopping conditions. Reference was made to brake application at the drive when stopping a downhill conveyor belt.

Surtees concluded that belts displaying low shock wave speeds are at higher risk of suffering high belt stresses than belts displaying high shock wave speed. - "the lower the speed is, the longer the waves take to decay".

He stressed the importance of starting system selection taking into account acceleration torque rate. He further suggested that belts should be allowed to come to rest freely during stopping but if brakes are needed they must be applied gradually or after a suitable interval after the drives have been de-energised.

Zür (1986) published a paper discussing mathematical models representing the relevant processes in the conveyor belt and drive during movement transients.

He described a Rheological model similar to that described by Nordell (1984) for computing the propagation velocity of the stress wave in the belt and for selecting the data concerning the take-up.

He concluded that the mathematical model enables the designer to determine the interactions between electromagnetic field, motor rotor, coupling, conveyor belt and take-up gear.

Figure 2.6 present a block-diagram of a general mathematical model of a belt conveyor as proposed by Zür.

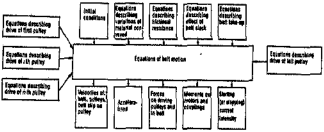

Figure 2.6 Block diagram of a discrete mathematical model of the belt conveyor (Zür, 1986).

During "Beltcon 4", a conference held by the South African Institute of Materials Handling and the South African Institute of Mechanical Engineers, several papers were presented on the subject of dynamic stresses in long conveyor belts.

Surtees (1987) discussed several case studies along the same lines as those presented in a previous paper by the same author.

Funke (1987) presented a short paper at Beltcon 4 describing the dynamic stress wave phenomenon.

Morrison (1987) addressed Beltcon 4 describing the results obtained from his finite element dynamic model of a conveyor. He presented graphic displays of three dimensional plots depicting stress waves. He discussed several case studies with the aid of three dimensional carpet plots of conveyor velocity behaviour during start up and shut down cycles. He demonstrated with the aid of carpet plots the effect of primary and secondary drives and belt loading on belt tension.

Morrison concludes that the model enables designers to have a complete picture of the tension and velocity dynamics for the whole belt as an aid in understanding behaviour of a conveyor system during the design process.

During "Beltcon 4", a conference held by the South African Institute of Materials Handling and the South African Institute of Mechanical Engineers, several papers were presented on the subject of dynamic stresses in long conveyor belts.

Surtees (1987) discussed several case studies along the same lines as those presented in a previous paper by the same author.

Funke (1987) presented a short paper at Beltcon 4 describing the dynamic stress wave phenomenon.

Morrison (1987) addressed Beltcon 4 describing the results obtained from his finite element dynamic model of a conveyor. He presented graphic displays of three dimensional plots depicting stress waves. He discussed several case studies with the aid of three dimensional carpet plots of conveyor velocity behaviour during start up and shut down cycles. He demonstrated with the aid of carpet plots the affect of primary and secondary drives and belt loading on belt tension.

Morrison concludes that the model enables designers to have a complete picture of the tension and velocity dynamics for the whole belt as an aid in understanding behaviour of a conveyor system during the design process.

Figure 2.7 is taken from Morrisons paper and illustrates the effects of start initiation of a double drive conveyor belt.

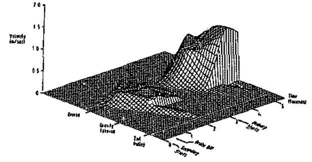

Figure 2.7 Velocity waves during start initiation (Morrison, 1987), note that the primary and secondary drives referred to in figure 2.7 relate to the physical installation rather than the start sequence.

The common aspect in all of the literature referred to is the total absence of standard solutions to the problem of dynamic stresses. It is clear that every belt installation needs to be studied and preventive action taken to minimise dynamic belt stresses.

None of the papers describe a case study of a belt profile similar to that of B18 conveyor at Goedehoop Colliery. The solution to the dynamic problems experienced in this conveyor belt therefore was to be found from a detailed study of the stresses as measured during field tests. Such tests had to be aimed at not only finding solutions for B18 conveyor but to produce design guidelines which would be applicable to the design of all long conveyor belt installations.

C H A P T E R   3

FIELD TEST PROGRAMME.

To solve the problems associated with this conveyor installation had to obtain a clear understanding of the stress waves with respect to their origins, magnitude and velocity had to be obtained. A test programme was conducted to measure a number of variables, details of which provided sufficient information to explain the phenomena.

3.1 PARAMETERS MEASURED.

The following measurements were taken simultaneously and plotted by high speed pen recorder for analysis.

Conveyor belt velocities in 4 places.

Belt load.

Belt tensions: at take-up and tail pulleys.

Take-up pulley movement.

Drive pulley torque during starting.

Brake pulley torque during stopping.

3.2 TEST EQUIPMENT.

The following equipment was used to conduct the tests:

4 Tacho generators to measure velocities.

Mass meter for belt load measurement.

2 Load cells for tension measurement

1 Potentiometer to measure take-up winch drum motion.

4 Strain gauge torque bridges.

Telemetry systems to transmit torque readings.

Tape recorders for field test data recording.

High speed pen recorders to provide graphic presentation of field test data.

Location of transducers to measure the above parameters are shown in figure 3.1.

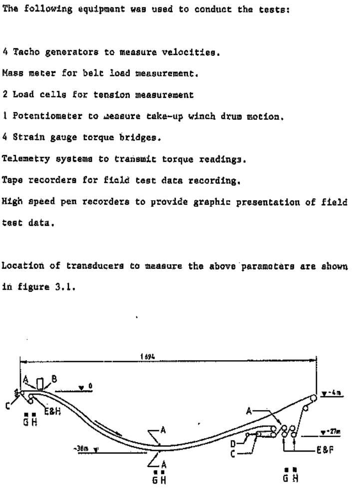

Figure 3.1 Location of measuring devices on B18 Conveyor.

3.3. TEST PROCEDURE.

Several test runs were undertaken in order to establish a no load reference and determine the conveyor system behaviour under varying load condition. A complete test comprised the recording of stopping and starting behaviour of the belt with all parameters at their standard settings for an empty belt, a partially loaded belt and a fully loaded belt. One parameter was then changed and the whole procedure was repeated to observe the effect of the parameter modification on all other parameters.

The following parameters were varied in turn:

Take-up pulley pre-tension .
Take-up pulley movement.
Starting sequence time delay between the two drive motors.
Braking torque.

Fach of the above parameters were modified several times to determine their optimum settings.

3.4 FIELD TEST LIMITATIONS.

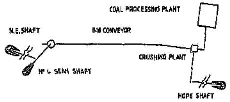

Figure 3.2 Surface Block Plan - Goedehoop Colliery.

The B18 conveyor installation is the main link between an important production area of the mine and the coal processing plant as shown in figure 3.2. The system was required to convey 6 000 tons of coal every day. Tests had to be performed in such a way that no production loss occurred. Modifications of parameters had to be conservative to allow sufficient safety margin to prevent breakdown of the system.

Distance also presented a constraint in performing the tests. Transducers were installed at various points along the length of the conveyor as shown in figure 3.1. Availability of mains power to drive recording equipment and measuring devices was the main problem.

A method to synchronise recorded results had to be developed. Hardwire or telemetry transmission of data were discarded because of its high cost and the possibility of volt drop and time delays associated with these methods. The problem was overcome by running a single pair of wires carrying a 24 Volt signal along the full length of the conveyor. The signal came on together with the application of power to the primary driving motor and fell away to zero volts when disconnecting the driving power. This signal was recorded at all stations along the belt. By matching the points of 24 volt switching on the different traces it was possible to accurately match recordings. The voltage signal velocity along the pair of wires corresponds to the speed of light i.e. approximately $1{,}7 \times 10^6$ metres per second. The time delay over 1 700 metres is therefore negligibly small in this instance.

The presence of stray currents and radio signals interfered with recording instruments. A 22kV powerline runs parallel to the B18 conveyor for at least 1km. This induces a 50 hertz 0,5 Volt stray current in the conveyor structure and therefore also in the power supply earthing. Measuring devices were operated at sufficiently high voltages to minimise the stray voltage effect. Radio signal interference occurred with telemetry equipment used to transmit driving and braking torque signals from shaft mounted strain gauges. Interference signals were tuned out to overcome the problem.

C H A P T E R 4

OBSERVATIONS AND RESULTS

Observations of belt behaviour on this project were divided into two main categories namely "shut down" and "start up" behaviour. High speed pen recorders were used to record results of all field tests. These graphs were interpreted as observations tabulated. The following tables summarise the observations. Test results will be discussed in Chapter 5.

Time (seconds) after stop initiation	Percent Full Load Driving Torque	
	Empty Belt	Loaded Belt
0,1	100	100
0,25	40	40
0,80	20	20
4	20	20
8	20	20
12	20	20
14	20	20
16	0	0

Table 4.1 Variation of driving torque with time after shut down initiation.

Maximum braking torque (kNm)	5	10
Time delay (seconds) to apply brakes	4,5	1,1
Time (seconds) to fully apply brakes	6,5	3,6
<u>Dynamic belt tension (kN)</u>		
At take-up: minimum	48	48
maximum	66	61
At tail pulley: minimum	48	48
maximum	59	66
Static belt tension after stopping (kN)	57	60
<u>Dynamic stress wave velocity (m/s)</u>:		
In empty return belt (V_R)	839	839
In loaded top belt (V_L)	385	385

Table 4.2 Effect of braking torque variation on dynamic stress wave intensity and velocity.

Belt loading (t.p.h.)	850	850
Braking torque (kNm)	5	10
<u>Average deceleration rate (m/s^2)</u>		
At drive	0,205	0,212
Return belt in valey	0,209	0,219
At tail pulley	0,209	0,215
Top belt in valey	0,212	0,218

Table 4.3 Effect of braking torque variation on belt deceleration rate.

Belt Load (t.p.h.)	0	850
Dynamic belt tension (kN):		
At take-up: minimum	48	48
maximum	57	66
At tail pulley: minimum	48	48
maximum	54	59
Static belt tension after stopping (kN)	57	57
Dynamic stress wave velocity:		
In return belt (m/s)	839	839
In top belt (m/s)	696	385
Time (seconds) to commence deceleration of top belt in valley	1,5	2,6
Average deceleration rate (m/s^2):		
At drive	0,217	0,205
Return belt in valley	0,231	0,195
At tail pulley	0,253	0,217
Top belt in valley	0,236	0,213

Table 4.4 Effect of load variation on B18 conveyor shut down behaviour.

Test Number	A	B
Belt loading (t.p.h.)	850	850
Winch reaction time (seconds)	0	1
Total winching out time (seconds)	0	8,2
Total winch rope travel (metres)	0	1,2
<u>Belt deceleration</u>:		
Average rate (m/s)	0,204	0,158
Total time to rest (seconds)	19,1	24,7
<u>Dynamic belt tension (kN)</u>:		
At take-up: minimum	48	48
maximum	66	63
At tail pulley: minimum	48	48
maximum	59	59
<u>Static belt tension after stopping (kN)</u>:	57	57

Table 4.5 Effect of inducing slack into the belt take-up during a loaded shut down cycle.

Secondary motor delay (sec)	7	14	27
Maximum torque (kNm)			
Primary drive	10	14	15
Secondary drive	23	21	11
Percentage of max. belt speed	6	37	93
Maximum acceleration rate (m/s^2)	6,67	1,84	0,98
Take-up belt tension (kN)			
Pre	39	36	36
Minimum	6	6	25
Maximum	48	52	39
Maximum tail pulley belt tension (kN)	47	48	43
Acceleration time (sec)	13	19	27,5
Time to settle down (sec)	45+	45+	37

Table 4.6 Effect of secondary drive delay variation during an empty belt start up cycle.

Load (T.P.H.)	Take-up Tension (kN) Minimum	Maximum	Tension Variance
0	37	51	14
440	21	59	38
726	5	57	52
850	9	66	57

Table 4.7 Effect of belt loading on take-up tension.

	Pre-tension (kN)	Dynamic Tension (kN) Minimum	Maximum	Tension Variance(kN)
(a)	40,9	6,7	47,7	41,0
(b)	42,6	5,2	51,0	45,8
(c)	44,9	10,8	47,7	36,9

Table 4.8 Effect of belt pre-tension variation on start up behaviour

C H A P T E R 5

DISCUSSION

The initial objective of this project was to investigate and analyse the dynamic shock waves in the belt during its stopping sequence. The investigation showed however that stopping cannot be considered in isolation.

The achievement of the smooth stopping of a conveyor system is only acceptable if the subsequent starting behaviour is within acceptable limits.

It is therefore necessary to also refer to start-up behaviour during the discussion of findings.

5.1 SOURCE OF DYNAMIC STRESS WAVES.

The main cause of shock waves in the belting is a sudden change in belt velocity.

5.1.1 System Inertia

Figure 5.1. illustrates the elements of the system inertia.

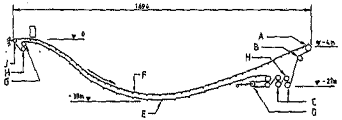

Figure 5.1. Conveyor mass distribution

A: Head Pulley

B: Bend Pulley

C: Drive Pulley

D: Take-up Pulley

E: Belt Carrying Idlers

F: Conveyor belting

G: Brake Pulley

H: Snub Pulleys

J: Tail Pulley

The belting is a long elastic band with evenly distributed mass, as shown in figure 5.1. Connected to the belt are a number of masses which influence its behaviour.

The idlers act as small rotating masses equadistantly spaced along the length of the belt - the top strand of the belt is supported by twice as many idlers as the return belt.

Snub, bend, head, tail and take-up pulleys are found at either end of the belt but more so at the drive end of the system. These are larger rotating masses concentrated in areas. Like the belt carrying idlers above they are also driven by the belt.

Drive pulleys in the case of the B18 conveyor are placed in the return strand of the belt near the head of the system. The two drive pulleys are connected through solid couplings to bevel gear reducers, the input shafts of which are connected through fluid couplings to 110kW motors. These rotating masses are the biggest in the system. They are different to all other masses in that they drive the belt to provide motion.

The brake pulley on B18 conveyor is installed in the return strand of the belt near the tail pulley. It has a brake drum attached to each shaft end which adds to its inertia. Braking is achieved when power is removed from the solenoids which keep the spring loaded brake shoes clear of the brake drums. The brake pulley is driven by the belt.

Each of the above has its own inertia with unique characteristics. The combination of these form the system.

Every belt installation will therefore display its own behaviour pattern.

From the above system inertia description it is clear that all of the masses attached to the belt will affect its behaviour. Because of the elasticity of the belt, high concentrations of inertia have the biggest impact

It will be shown that belt carrying idlers have a damping effect on the stress wave velocity but because of its even distribution and relatively small size plays no role in the initiation of the shock wave.

Snub, bend, head, tail and take-up pulleys also have a relatively small inertia compared to that of the system and do not have a significant influence upon the generation of shock waves.

Figure 5.2. shows the drive system, the main cause of shock wave generation in the system. It has a large concentrated inertia. While driving the belt it exerts high tension, T_1 on the loaded side of the belt while the return side is being kept tight by the take-up winch exerting a pre-determined tension, T_2.

Under steady running conditions the tension differential across the drive pulleys is a constant 34kN.

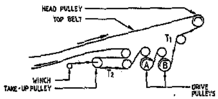

Figure 5.2 Typical double drive conveyor under steady running conditions.

At the instant when the driving power is removed the belt becomes the driving force with the drive pulleys forming a lumped high inertia driven load. The immediate effect is a sudden stress reversal in the belt across the drive pulley with the high tension stress switched to the take-up side of the drive. This initiates a stress wave which propagates along the return belt to the tail pulley as shown in figure 5.3.

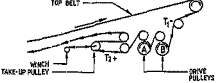

Figure 5.3 Effect immediately after power cut to drive pulleys.

From figures 5.2 and 5.3 it is seen that the tension in the take-up belt increases immediately after the power cut to the drive pulleys due to the belt now becoming the driving force and 2,3 seconds later the same effect is detected at the tail pulley, as shown in figure 5.4.

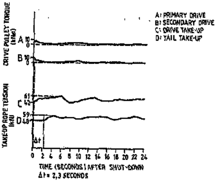

Figure 5.4 Effect of changing the drive pulleys into a high inertia driven load.

The sudden addition of the high inertia drive train to the work done by the elastic belt is therefore one of the big contributing factors to the generation of the dynamic tensile stress wave in the return belt of the conveyor system. The au'or believes that the addition of a high inertia flywheel to each of the drive gearbox high speed shafts will largely eliminate the abrupt change from driving force to driven inertia and thereby prevent the generation of the stress wave as described above.

Others have suggested a controlled stopping action by gradually reducing driving torque through the addition of rotor resistance into the driving motors. This proposal is only effective as long as power is available at the drive motors. When a power trip is experienced the above controls are lost and driving torque is again removed instantaneously.

5.1.2 Local belt velocity variation.

Because of the elastic properties of the belting used on belt conveyors, it is to be expected that velocity variations will be present along the length of the belt even during steady running conditions.

During steady running conditions the belting comes into contact with items of different inertia and also passes through the drive section changing tensions as discussed in section 5.1.1.

Load variations on the top belt and between top and return belts also cause tension variations.

These tension variations result in local belt velocity variations as shown in figure 5.5.

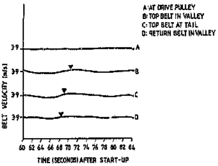

Figure 5.5 Belt velocity variation under steady running conditions of B18 Conveyor loaded to 850 tons per hour.

Figure 5.5 illustrates not only the local velocity variations during steady running conditions but also the propagation of the high velocity wave in an opposite direction to that of the belt travel.

During the stopping cycle the same phenomena are present but much more pronounced as shown in figure 5.6.

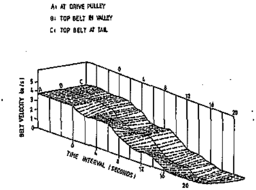

Figure 5.6 Three dimensional plot of belt velocity at three points along B18 conveyor during an 850 tons per hour stop with no braking torque applied.

Figure 5.7 illustrates what happens during an acceleration cycle at 850 tons per hour and figure 5.8 for an empty condition.

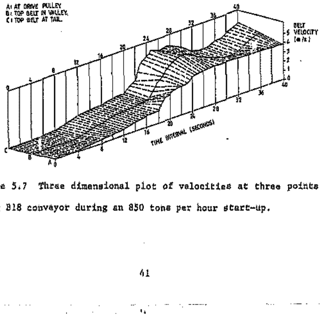

Figure 5.7 Three dimensional plot of velocities at three points along B18 conveyor during an 850 tons per hour start-up.

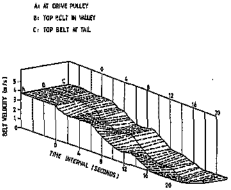

Figure 5.6 Three dimensional plot of belt velocity at three points along B18 conveyor during an 850 tons per hour stop with no braking torque applied.

Figure 5.7 illustrates what happens during an acceleration cycle at 850 tons per hour and fi‿ure 5.8 for an empty condition.

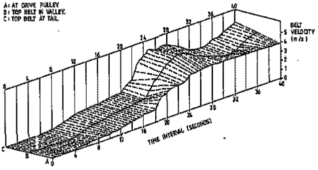

Figure 5.7 Three dimensional plot of velocities at three points along B18 conveyor during an 850 tons per hour start-up.

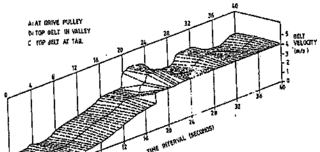

Figure 5.8 Three dimensional plot of velocities at three points along B18 conveyor during an empty start-up.

Figure 5.9 illustrates the propagation of a velocity wave along the belt and the transformation of the velocity change at point C, at the tail end into tension which, when measured at the take-up pulley, Point A, is identical in shape, but displaced in time, to the velocity graph.

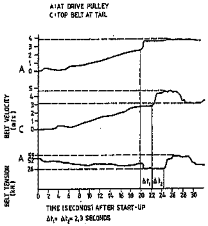

Figure 5.9 Comparison of belt acceleration at the drive with belt velocity at the tail and tension at the take-up pulley during an empty start.

The equivalent comparison during a starting cycle when the belt carried 850 tons per hour is shown in figure 5.10

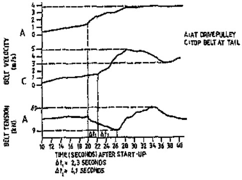

Figure 5.10 Comparison of belt acceleration at the drive with belt velocity at the tail and tension at the take-up pulley during an 850 tons per hour start-up cycle.

Figure 5.11 shows the relationship between *velocities* and tensions at the drive and tail sections of the belt during a stopping cycle under loaded conditions.

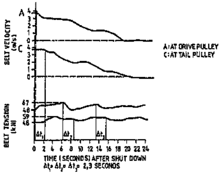

Figure 5.11 Relationship between belt velocities and tensions during a shut-down cycle with belt load at 850 tons per hour.

From the above it is clear that a sudden belt velocity change at one point converts into a dynamic stress wave transmitted throughout the entire belt length at high speed in the opposite direction to the belt travel.

Prevention of the stresses caused by velocity is similar to that described in section 5.1.1 namely the utilisation of "soft" start and controlled stop systems.

5.2. SHUTDOWN BEHAVIOUR OF B18 CONVEYOR.

Having studied the origin of the dynamic stress waves in B18 conveyor, it was necessary to determine the inter-relationship of the variable parameters of the system. Several options were identified to alter the behaviour of the dynamic stresses in the belting.

The shutdown cycle of the system is initiated by the removal of the conveyor driving power. In the case of B18 conveyor at Goedehoop Colliery this occurs suddenly by cutting the electric supply to both driving motors.

Harrison (1985) showed that dynamic stress is proportional to instantaneous belt velocity. He recommended the use of wound rotor resistance control to apply and remove driving torque in acceptably small increments. While the author recognises the effectiveness of this solution to prevent the initiation of shock waves, it is necessary to point our that it ·ssumes the availability of electric power at all times during a shut down cycle. Conditions exist in practice where electric power to the driving motors is totally lost for example during a total power outage to the complex or during an electric fault condition in the conveyor driving or control systems.

Safe operation of conveyor systems also requires that emergency shut down brings the belt to a stop in the shortest possible time.

The design of a conveyor system must therefore cater for the sudden removal of electric driving power to the driving motors of the system.

Shut down variations studied on B18 conveyor included alterations to braking torque, belt loading, and take-up tension.

5.2.1 Effect of varying braking torque.

The B18 conveyor at Goedehoop Colliery was equipped with a brake pulley in the return belt immediately before the conveyor tail end as shown in figure 5.12.

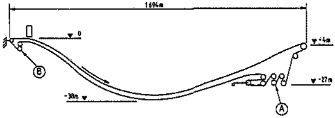

Figure 5.12 Cross section of B18 Conveyor.

A: Drive Section.

B: Brake Pulley.

The drum brakes attached to the brake pulley shaft were electric solenoid released and spring applied failing to safety, i.e.

brakes on with loss of electric power. Variation of braking torque were obtained by adjusting the brake shoe travel.

Figure 5.13 illustrates the belt behaviour as measured in terms of velocity and tension at several points along the belt during an 850 tons per hour shut down with minimum braking torque applied.

Figure 5.14 compares the same measurements during an 850 tons per hour shut down when maximum braking torque is applied.

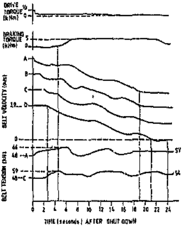

Figure 5.13 Behaviour of belt velocity and tension during an 850 tons per hour shut down with minimum braking torque applied at the tail end of B18 conveyor.

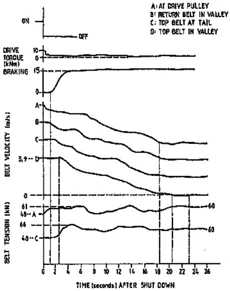

Figure 5.14 Effect of high braking torque applied at the tail end of B18 conveyor on belt velocity and belt tension during an 850 tons per hour shut down.

In both cases the driving torque of one motor only is shown since both motors behave the same namely a reduction of 60% of full load torque in 0.25 seconds and 80% of full load torque in 0,8 seconds after which the inertia of the drive continues to maintain 20% torque for another 13 seconds.

Figure 5.13 shows the application of brakes at 4,5 seconds after shut down when braking torque builds up to 5 kNm in 2 seconds whilst in the case of figure 5.14 brakes are applied at 1,1 seconds and braking torque reaches 15 kNm in another 2,5 seconds.

Table 5.1 shows the comparative belt deceleration rates for the two conditions at various points along the belt as indicated on figure 5.15 and referred to in figures 5.13 and 5.14

A: At the drive pulley.

B: Return belt in the valley.

C: Top belt at the tail.

D: Top belt in the valley.

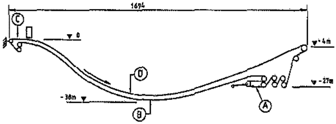

Figure 5.15 Tachometer locations along B18 conveyor.

Location	Minimum Braking Av. Deceleration rate (m/s^2)	Maximum Braking Av. Deceleration rate (m/s^2)
A	0,205	0,212
B	0,209	0,219
C	0,209	0,215
D	0,212	0,218

Table 5.1 Comparison of deceleration rate of the Goedehoop B18 conveyor during an 850 tons per hour shut down with variation of braking torque.

Referring to figures 5.13 and 5.14 [illegible] table 5.1, the following observations were made:

(i) Local velocity variations were less intense with maximum braking torque applied.

(ii) The higher braking torque assisted to eliminate the velocity surges of the loaded belt in the valley with consequent spillage reduction.

(iii) Peak belt tension at the drive was lower at 61 kN compared to 66 kN with higher braking torque at the tail end of the belt.

(iv) Belt tension fluctuation at the drive was less with the higher braking torque.

(v) The drive take-up tension was higher after the belt came to rest (60kN compared to 57kN) with the higher braking torque. This is advantageous for the following start up cycle to reduce dynamic stresses during the start up cycle.

(vi) Peak belt tension at the tail was higher at 66kN compared to 59kN, with increased braking torque. This largely offsets the advantage gained by reduced belt tension at the drive pulleys.

(vii) Time taken for the dynamic stress wave to travel the 1678 metres between points A and C along the return belt was 2 seconds, which gave a stress wave velocity, V_R, of 839 metres per second along the return belt.

(viii) Time taken for the dynamic stress wave to travel the 1810 metres along the loaded top belt from C via D to A was 4.7 seconds, which gave a stress wave velocity, V_L, of 385 metres per second along the loaded top belt. This lower stress wave velocity is due to the damping effect of the load on the belt and the additional carrying idlers in contact with the top belt referred to in section 5.1.1.

5.2.2 Effect of belt loading.

It was shown in the previous section that belt loading had a significant damping effect on the dynamic stress wave velocity. Figures 5.16 and 5.17 compare the shut down behaviour of the B18 conveyor under empty and carrying 850 tons per hour conditions respectively.

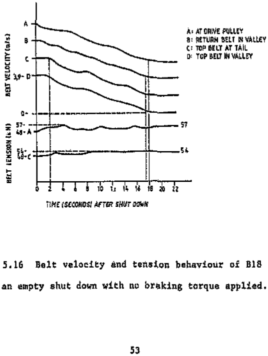

Figure 5.16 Belt velocity and tension behaviour of B18 conveyor during an empty shut down with no braking torque applied.

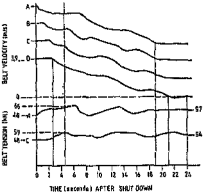

Figure .5.17 Behaviour of belt velocity and tension of B18 conveyor during an 850 tons per hour shut down with no braking torque applied.

Observations.

(i) Belt tensions did not fluctuate much during the empty shut down when compared to that of the loaded belt.

(ii) Maximum belt tension measured at the take-up pulley during an empty shut down was 57kN whilst at the tail pulley only 54 kN was measured.

(iii) A fairly constant rate of deceleration was measured during the empty shut down with the exception of point C at the tail end of the belt where a slight fluctuation was detected.

(iv) The dynamic stress wave velocity along the return belt, V_R, from A via B to C was the same under both sets of conditions namely 839 metres per second as before. The load on the top belt had no effect on the dynamic stress wave velocity in the return belt.

(v) The dynamic stress wave velocity in the empty top belt V_E shown in figure 5.16 was however significantly higher at 696 metres per second than was the case for the loaded top belt shown in figure 5.17. As before the dynamic stress wave velocity in the belt loaded at 850 tons per hour, V_L, was 385 metres per second. The explanation for the differences between V_R, V_E and V_L is:

a. The damping effect of belt carrying idlers. The top belt is carried by 1453 idlers and the return belt by 363. Whilst both top and return belts were therefore empty the damping effect of the idlers resulted in a reduction of dynamic stress wave velocity from V_R = 839 metres per second to V_E = 696 metres per second.

(b) The damping effect of the 850 tons per hour load carried by the belt which caused a further reduction from V_R = 696 metres per second to V_L = 385 metres per second.

See annexure C for theoretical stress wave velocity calculations.

(vi) Referring to figure 5.17 a clearly defined secondary dynamic belt stress wave initiated at point D 2,6 seconds after shut down when deceleration commenced at this point. This dynamic stress wave travelled opposite in direction to the initial stress wave which travelled in the same direction as the belt.

Secondary stress waves in belts normally result from partial reflections of a primary wave as it passes through the drive. In the case of B18, however, the loaded downhill belt section attempted to "overtake" the loaded uphill belt section. This resulted in momentary slack belt in the valley. At 2,6 seconds after shut down the primary stress wave had reached point D, causing sudden decelleration of the belt at this point. This caused a jerk to the belt as the slack belt in the valley pulled tight and initiated the secondary shock wave travelling back along the belt. Figure 5.18 is a carpet plot of belt velocities illustrating the primary and secondary dynamic stress wave fronts generated in the belting during an 850 tons per hour shut down cycle.

Further stress waves are also seen on the plot, however these are contaminated due to interaction between the initial waves and reflections from the major pulleys in the system.

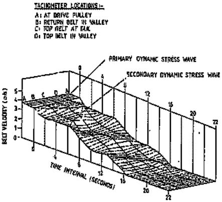

Figure 5.18 Dynamic stress waves in B18 conveyor belting during an 850 tons per hour shut down cycle.

The carpet plot shown in figure 5.18 and others in this report relate space, time and belt velocity to each other. They were derived from simultaneous measurement of velocities at points a,b,c, and d along the belt. Velocities were recorded continuously but plotted every 0,25 seconds along the X-axis. Points representing the same time value were then connected with straight dotted lines to illustrate the velocity waves. Accurate belt velocities are therefore only represented along the continuous velocity traces shown on the carpet plots. Figure 5.9. and 5.10 in section 5.1.2 of this report illustrated the direct relationship between belt velocity wave propagation and stress wave propagation hence the reference in figure 5.18 to dynamic stress waves whilst technically we have velocity waves.

5.2.3 Inducing slack into the take-up system.

The dynamic shock wave during a shut down cycle was initiated by the sharp drop in velocity of the drive system immediately after shut down initiation. This resulted in a sharp increase in belt tension in the take-up section immediately behind the belt drive shown in figure 5.19.

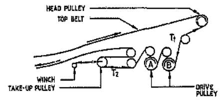

Figure 5.19 Modified drive and take-up arrangement of B18 conveyor.

The introduction of slack into the belt in the take-up area was attempted to counteract the tension build-up in the belting at that point. This was achieved by replacing the gravity take-up with a winch take-up and allowing the take-up winch to pay out rope to the take-up pulley for a period in excess of the first dynamic tension cycle in the belting in the take-up area. Figure 5.20 shows the results of one such test when the take-up winch paid out slack for 8,2 seconds after initiation of the shut down cycle when the conveyor carried 850 tons per hour.

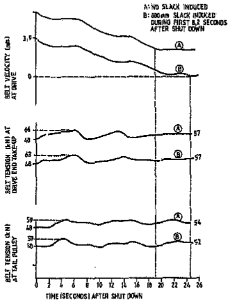

Figure 5.20 Introduction of slack into the drive take-up of B18 conveyor during an 850 tons per hour shut down cycle.

Observations.

(i) No significant change was detected at the tail pulley.

(ii) The introduction of slack resulted in a reduced peak stress of 63kN from 66kN in the take-up area as shown in figure 5.20 (b).

(iii) Final belt stresses after the belt had come to rest remained unchanged in the take-up area at 57kN but slightly reduced in the tail end area of the belt at 52kN from the previous 54kN.

(iv) No change took place in the stress build up during the first second after shut down initiation. This is due to the slow reaction time of the winch. It can be seen in figure 5.20 (b) that a significant change in stress build up at the take-up occurs after the first second when the winch gets up to full speed.

(v) With the introduction of slack the belt deceleration pattern was slightly smoother and the belt took 5,6 seconds longer to come to rest as shown in figure 5.20 (a).

Shutdown behaviour of B18 conveyor was found to be controllable by application of brakes at the tail of the belt and introduction of slack at the take-up pulley.

Braking is standard practice in many installations but has a negative effect on the system reliability. Some of the most common failures of braking systems are worn brake pads and binding brakes. In addition incorrectly set brakes can result in severe dynamic stress generation at the tail pulley of the conveyor.

Introduction of slack at the take-up pulley at the moment of shut down initiation has not been applied to date as far as the author could establish. The take-up winch reacts too slowly to provide this slack.

The author proposes that further research should be carried out to design a system of stored tension which can be released with a reaction time of 0,1 second and for long enough to arrest the initial stress build-up after shut down. The end of the "slack pay-out cycle" should also be gradual to prevent initiation of yet another shock wave into the system. Care should also be taken to limit the amount of slack released into the system since too much slack will prevent proper pre-tensioning of the belt and will result in severe dynamic stresses induced in the belt during the subsequent start up cycle.

5.3 START UP BEHAVIOUR OF B 18 CONVEYOR.

The Goedehoop Colliery B18 conveyor starting cycle operates as follows:

(i) The control system will allow a belt start if the safety circuit comprising field emergency stop switches, equipment sequence interlocking, and oil cooling system are healthy.

(ii) Start button is pressed.

(iii) The take-up winch winds in to adjust the belt tension to the "pre-start" value.

(iv) Brakes lift off.

(v) The primary drive starts. This drive is equipped with a high speed scoop controlled fluid coupling. The coupling scoop tube winds in at a pre determined rate to control the oil supply to the coupling which in turn regulates the primary drive torque build-up.

(vi) The secondary drive which is equipped with a delay fill fluid coupling is driven by the belt through its gear reducer and fluid coupling. At a pre-selected time delay after the primary drive start-up, the secondary drive starts and runs up to full speed. The delay fill fluid coupling has an internal regulator which regulates oil flow from storage to operating chambers inside the coupling. Oil flow in this coupling is sustained by centrifugal force.

(vii) When the belt is up to full speed the take-up winch winds out to reduce belt tension to a pre-selected "running tension".

Start-up tests were performed on this conveyor to observe the effects of adjusting the delay time between drives, belt loading, and take-up pre-tensioning.

5.3.1 Start-up delay variation.

The design specification for B18 conveyor called for a seven second delay between primary and secondary drive start initiation.

Figure 5.21 shows a satisfactory acceleration curve under loaded conditions for both a seven second and a 26,5 second time delay start-up. This figure also shows similar behaviour of belt tension at the belt take-up area. The design therefore specified the shorter start-up cycle in order to prevent unnecessary temperature build-up in the fluid couplings. A complete analysis of the loaded start will be done in a later section.

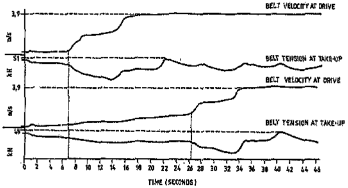

Figure 5.21 Time delay variation between the two drives of B18 conveyor and its effect on belt acceleration and take-up tension during a 700 tons per hour start-up cycle.

What seemed in order for starting under loaded conditions proved to be unacceptable for starting an empty belt. Figures 5.22, 5.23 and 5.24 show the behaviour of all the belt start test parameters which were monitored for three different drive delay conditions namely seven second delay, fourteen and twenty seven seconds delay.

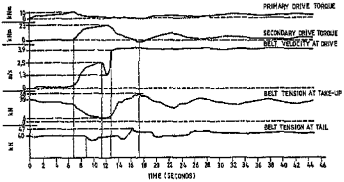

Figure 5.22 Empty belt start-up with seven seconds delay between primary and secondary drive motors activation.

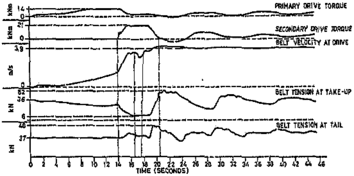

Figure 5.23 Empty belt start-up with 14 seconds delay between primary and secondary drive motors activation.

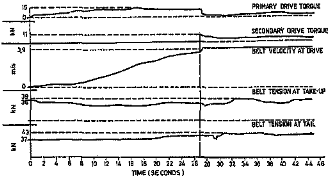

Figure 5.24 Empty belt start-up with 27 seconds delay between primary and secondary drive motors activation.

Table 5.2 summarises some of the important values read from figure 5.22, 5.23 and 5.24.

Secondary motor delay (sec)	7	14	27
Maximum torque (kNm)			
Primary drive	10	14	15
Secondary drive	23	21	11
Percentage of max. belt speed	6	37	93
Maximum acceleration rate (m/s^2)	6,67	1,84	0,98
Take-up belt tension (kN)			
Pre-start	39	36	36
Minimum	6	6	25
Maximum	48	52	39
Maximum tail pulley belt tension (kN)	47	48	43
Acceleration time (sec)	13	19	27,5
Time to settle down (sec)	45+	45+	37

Table 5.2 Empty belt start up with different time delays for secondary drive start initiation.

Figure 5.25 shows the maximum torque variation of the two drives when starting B18 conveyor with varying time delays between drives under empty conditions.

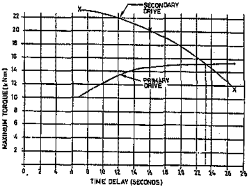

Figure 5.25 Maximum torque variation with time delay between primary and secondary drives when starting B18 conveyor empty.

Observations.

(i) A time delay of approximately 23 seconds gave equal maximum torque transmitted by drives during start-up under empty conditions.

(ii) The shorter time delay required excessively high power input from the secondary drive which in turn generated large dynamic stresses in the belting. This was confirmed by the very high rate of acceleration of 6,67 metres per second measured with the seven second time delay compared to 0,98 metres per second with the 27 second time delay.

(iii) Take-up belt tension fluctuations were much smaller at 14 kN maximum with the 27 second time delay compared with the shorter ones at 42 and 46 kN respectively.

(iv) Belt slip occurred during both the seven and fourteen second time delay starts. This is seen in figure 5.22. at 11 seconds and figure 5.23 at 16.5 seconds This slipping was the main reason for the high rate of belt acceleration seen with the seven second delay and the wild take-up tension fluctuations with the seven and 14 second time delay starts.

(v) It was noticeable that the belt settled down within 10 seconds after the second motor came on at 27 seconds whilst in both other tests with the shorter time delays the surging continued for a long time.

The longer delay time before starting the secondary drive therefore suited the B18 installation. The external oil coolers of the scoop controlled fluid coupling proved to be effective in preventing oil overheating.

Replacing the delay fill fluid coupling of the secondary drive with a double delay fill coupling would enable a safer start with a shorter delay between drives.

The effectiveness of the fluid coupling in the secondary drive was largely lost because this drive was driven by the belt prior to activation of the secondary drive. This meant that by the time it came on line a large quantity of the oil had flown from the storage chamber into the working compartment of the coupling. These couplings work on the assumption that the motor starts with no load and oil flow into the working compartment provides a smooth load transition to the motor. It is obvious from the above that this advantage is partly lost with secondary and subsequent drives after the belt had started moving as would be the case with empty belts.

5.3.2. Effect of belt load on start up dynamic shock loads.

Reference was made in section 5.3.1 to the fact that the loaded belt acceleration pattern showed little variation between shorter and longer inter-drive start up delays.

Table 5.3 shows a comparison of belt tension in the take-up area for various load conditions.

Load	Take-up Tension (kN)		Tension
(T.P.H.)	Minimum	Maximum	Variance
0	37	51	14
440	21	59	38
726	5	57	52
850	9	66	57

Table 5.3 Take-up tension variation during start up for various load conditions on B18 conveyor.

From the above table it is seen that:

(i) The shock wave was initiated in every case by the activation of the secondary drive.

(ii) The peak value the shock wave was proportional to the load carried on the belt.

Figure 5.26 is a carpet plot of B18 conveyor belt velocities under loaded conditions and figure 5.27 for an empty belt. Note the presence of a small shock wave immediately after start initiation of the belt and the instantaneous velocity change when the secondary drive was activated at 18 seconds in figure 5.27. Violent shock waves are clearly seen in the following 20 seconds.

The acceleration rate of the loaded belt in figure 5.26 was reduced compared to that of the empty condition and this was followed by a lower velocity shock wave after the activation of the secondary drive.

A comparison of peak velocities, which in both cases occurred at the tail pulley showed that the loaded belt reached a velocity of approximately 5 metres per second and the empty belt approximately 4,5 metres per second. The corresponding belt tensions were 69 kN and 59 kN respectively.

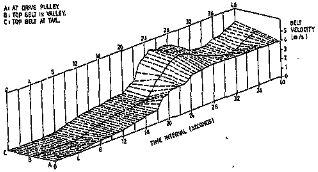

Figure 5.26 Carpet plot of B18 conveyor belt velocities for a loaded start.

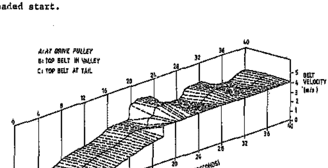

Figure 5.27 Carpet plot of B18 conveyor belt velocities for an empty start.

From the above it would seem as if the loaded belt with its lower acceleration rate should have suffered lower dynamic stresses than the empty belt with its violent velocity change. The advantage of the slower acceleration of the loaded belt in the case of B18 conveyor is however counteracted by the catenary shape of the conveyor. The downhill section of the belt is assisted by gravity during acceleration, hence the magnification of the acceleration rate of the belt towards the tail section and the resulting higher dynamic stresses.

5.2.3. Effect of belt pre-tension on start up behaviour

Harrison (1986) proposed optimisation of pre-tensioning of the belt take-up prior to start initiation as a method of limiting dynamic stresses during start up. This theory was tested on *B18 conveyor*. The results are shown in table 5.4.

	Pre-tension (kN)	Dynamic Tension (kN) Minimum	Maximum	Tension Variance (kN)
(a)	40,9	6,7	47,7	41,0
(b)	42,6	5,2	51,0	45,8
(c)	44,9	10,8	47,7	36,9

Table 5.4 Effect of pre-tension variation on dynamic stresses during a 730 tons per hour start.

Harrisons theory is not confirmed by the results tabulated above. Test (b) should however be discarded since belt slip occurred when the take-up tension dropped as low as 5,2 kN. This may explain the subsequent unexpectedly high maximum tension.

A comparison of tests (a) and (c) in table 5.4 then confirms the theory that a higher pre-tension results in a smoother start up cycle with lower dynamic stress variation.

This phenomenon is the main reason why conveyor shut down behaviour and methods of reducing dynamic stresses during shutting down cannot be viewed in isolation. It was shown before that releasing slack into the take-up belt resulted in a smooth stopping action with minimal dynamic stresses in the belt. The test in question was the one preceeding the test in table 5.4 (a). As seen above the consequence of the improved stopping achieved by excessive slack induction, was aggravation of dynamic stresses during the following start cycle.

For the same reason it is not advisable to alter any parameter of the conveyor control mechanisms without confirming its effect on the behaviour of all the other parameters.

CHAPTER 6

CONCLUSIONS AND RECOMMENDATIONS

6.1 CONCLUSIONS.

Dynamic stresses in B18 conveyor at Goedehoop Colliery were found to be initiated both during starting and stopping from the rate of applying and removing the conveyor driving power.

The catenary shape of the overland conveyor complicates the belts dynamic stress behaviour, but was not found to be the source from which dynamic stress waves were initiated.

The braking system installed at the tail-end of the conveyor had a damping effect on circulating dynamic stresses during the shut down cycle. At the same time the application of brakes increased the belt tension at the tail pulley. Brake adjustment for braking torque and rate of application proved to be critical. Poor maintenance of brakes can result in brakes binding during normal running of the belt and an excessive braking torque applied during stopping. This in turn will initiate destructive dynamic stresses at the tail end of the belt during the stopping cycle.

The winch controlled take-up which replaced the gravity take-up system on 818 conveyor proved to be successful in withstanding the large circulating stresses in the belt. It also served a useful purpose to provide sufficient pre-tensioning of the belt for the sta .ing cycle - a factor which served to reduce peak stresses in the belting. During stopping cycles the winch was successfully employed to release initial stress build up in the take-up belt which in turn dampened the circulating dynamic stresses in the conveyor belt.

The load carried by the belt had a damping effect on the stress wave velocity. This made stress peaks during starting less critical. At the same time, however, belt loading increased dynamic stress peaks during the stopping cycle, a phenomenon which limited the 818 belt safe carrying capacity to 800 tons per hour. The use of brakes at the tail end of the conveyor allowed a safe carrying capacity of 1 000 tons per hour which was in line with the designed capacity of the system.

Controlling the application and removal of belt driving power of this installation was limited to variatio of the scoop controlled coupling torque build up and the time interval between initiation of primary and secondary drives. The primary scoop controlled coupling drive was never a factor in the generation of dynamic stresses whilst the delay fill hydraulic coupling secondary drive proved to be the source of dynamic stresses during the starting cycle. The timing between drives initiation was not as critical when starting a loaded belt from the point of stress generation as was the case when starting an empty belt. A far greater time delay than that recommended by the equipment suppliers proved to be the optimum setting to give satisfactory start up behaviour under loaded and empty conditions.

Controlled driving torque removal during stopping was ruled out as a means of reducing dynamic stress peaks. Whilst the effectiveness of the method is recognised by the author the practicality of it is questioned in the case of the B18 conveyor installation. This conveyor is at the rear end of a whole train of equipment that is all sequence interlocked which means that any item stopping ahead of B18 conveyor would result in an emergency stop of B18. In addition B18 is fitted with emergency devices which again could cause emergency stops. It is therefore necessary to ensure that the system design should cater for the condition when all driving power is removed instantaneously as is also the case during a total power failure.

6.2 RECOMMENDATIONS.

Dynamic stress waves in the belting of this conveyor installation will never be entirely eliminated. Steps can be taken to minimise these stresses.

6.2.1 Braking system.

The present braking system is to be maintained in order to enable the belt to carry the system designed capacity of 1 000 tons per hour. Care should be taken that brakes are correctly adjusted at all times to operate effectively without inducing excessive belt stress at the tail-end of the belt.

6.2.2. Shock absorbing system.

Releasing slack into the belt take-up during stopping proved to be partly successful in absorbing the shock wave initiated by the sudden removal of driving power. Further research in this area should be done to develop a system capable of releasing the required slack with a response time of 0,1 second as discussed in section 3.2.3.

6.2.3. Pre-tensioning.

The winch take-up control system on this conveyor must be maintained to provide a belt pre-tension of between 45 kN and 50 kN before the belt start-up sequence is initiated. This will assist in limiting dynamic stress build up during belt start-up. Once the belt is up to full speed the take-up tension can be released to between 25 kN and 35 kN.

The reason for giving a range within which to operate take-up tension is to prevent hunting of the winch whilst attempting to control to a single set point. It was shown previously that belt tension varies all the time during full speed running conditions.

It should not be attempted to control belt tension with the winch during the shut down cycle. Apart from the fact that the winch reaction time is far too slow to follow dynamic stress waves passing through the take-up area, there is also a real danger that winch movement during shut down could oppose a dynamic stress wave passing over the take-up pulley resulting in instantaneous doubling of the peak stress value. This could in turn cause snapping of the conveyor belt.

6.2.4 Drive starting torque.

The present drive configuration of primary drive with scoop controlled fluid coupling and secondary drive with delay fill fluid coupling is unsatisfactory.

The time delay between primary and secondary drives starting under these conditions must be between 20 and 30 seconds to minimise dynamic stress generation.

It is recommended to replace the secondary drive delay fill fluid coupling with a double delay fill fluid coupling to reduce the unsatisfactory rapid torque build-up rate, when this drive is started, to an acceptable level.

Such a modification will also enable a shorter delay between primary and secondary drives starting.

REFERENCES.

Funke, H (1987) "Longitudinal Vibrations during Transient Operating Conditions of Belt Conveyors" Beltcon 4, South Africa (1987).

Harrison, A (1985) " Reducing Dynamic Loads in Belts powered by the Three Wound Rotor Motors" Bulk Solids Handling, Volume 5, Number 6 (1985), pp 73-77.

Harrison, A (1986) " Stress Front Velocity in Elastomer Belts with Bonded Steel Cable Reinforcement" Bulk Solids Handling, Volume 6, Number 1 (1986) , pp 79-83.

Harrison, A and Roberts, A.W. (1983) "Technical Requirements for operating Conveyor Belts at High Speed " Bulk Solds Handling, Volumes 4, Number 1 (1984), pp 99-104.

Surtees, A J (1987) "Longitudinal Stresses Occurring in Long Conveyor Belts during Starting and STopping" Bulk Solids Handling, Volume 6, Number 4 (1986), pp 93-97.

Surtees, A J (1987) "Further Case Studies in Transient Stresses in Belt Conveyors "Beltcon 4, South AFrica (1987).

Zür, T W (1986) "Viscoelastic Properties of conveyor Belts "Bulk Solids Handling, Volume 6, Number 3 (1986), pp 553-560.

Morrison, W R B (1987) "Computer Graphics Techniques for Visualising Belt Stress Waves" Beltcon 4, South Africa (1987).

Nordell, L K (1987) "The Theory and Practice of Belt Conveyor Dynamic Analysis" Beltcon 4, South Africa (1987).

Nordell L K and Ciozda Z (1984) "Transient Belt Stresses During Starting and Stopping: Elastic Response Simulated by Finite Element Methods "Bulk Solids Handling, Volume 4 Number 1 (1984), pp 93-98.

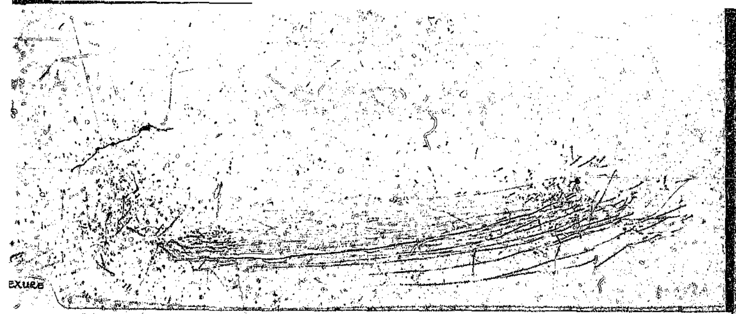
EXURE

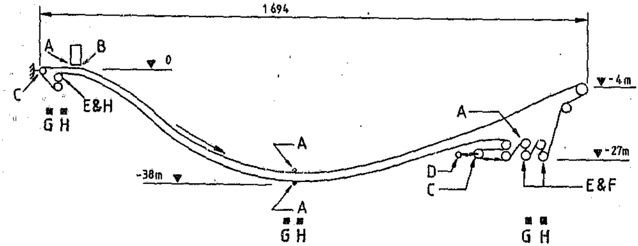

FIG 3·1 LOCATION OF MEASURING DEVICES ON B18 CONVEYOR

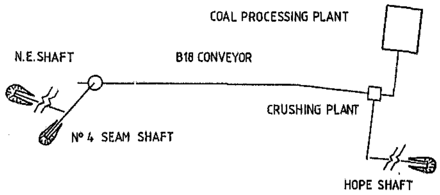

FIGURE 3·2 SURFACE BLOCK PLAN-GOEDEHOOP COLLIERY

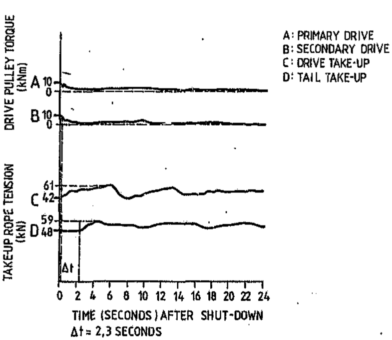

FIGURE 5·4 EFFECT OF CHANGING DRIVES INTO A HIGH INERTIA DRIVEN LOAD

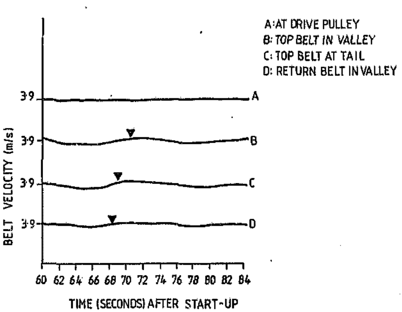

FIGURE 5·5 BELT VELOCITIES UNDER STEADY RUNNING CONDITIONS

A: AT DRIVE PULLEY

B: TOP BELT IN VALLEY

C: TOP BELT AT TAIL

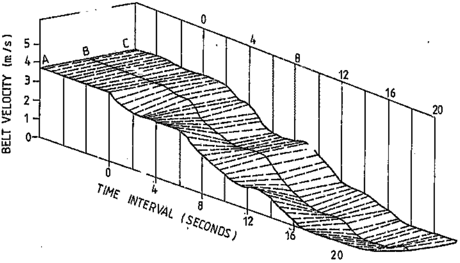

FIGURE 5.6 CARPET PLOT OF CONVEYOR B18-VELOCITIES DURING A LOADED STOP

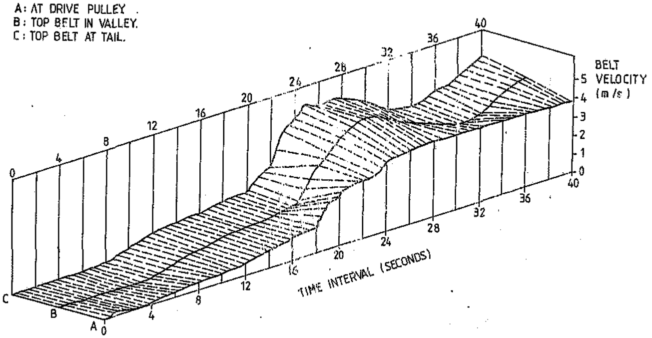

FIGURE 5.7 CARPET PLOT OF B18 CONVEYOR VELOCITIES DURING A LOADED START.

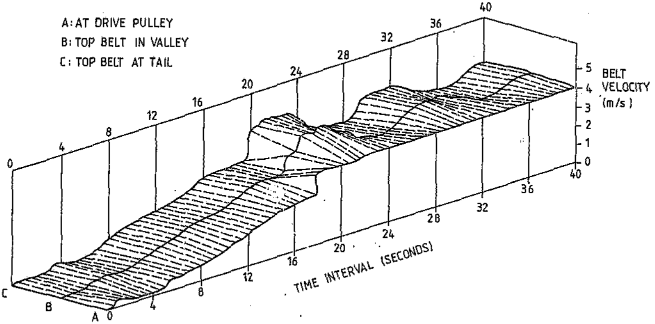

FIGURE 5·8 CARPET PLOT OF B18 CONVEYOR VELOCITIES DURING AN EMPTY START.

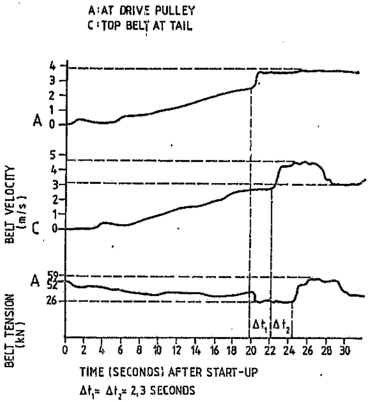

FIGURE 5·9 BELT VELOCITY WAVE CONVERSION TO A TENSION WAVE-EMPTY START

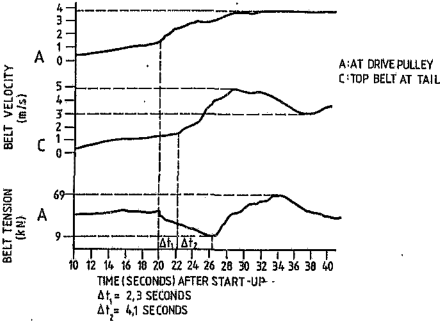

FIGURE 5·10 BELT VELOCITY WAVE CONVERSION TO A TENSION WAVE-LOADED START

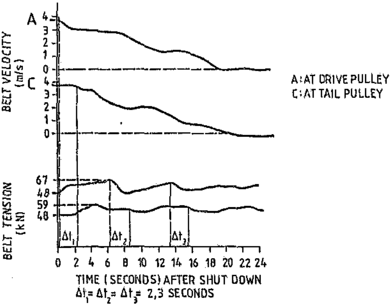

FIGURE 5·11 BELT VELOCITIES AND TENSION RELATIONSHIPS-LOADED STOP

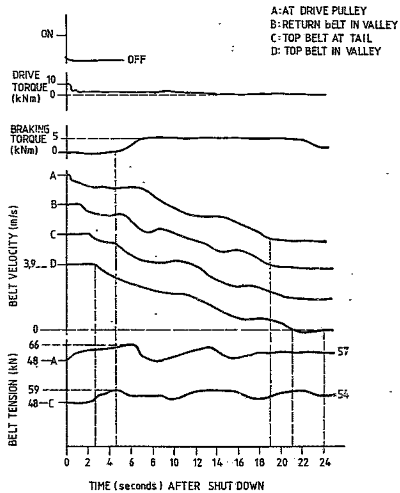

FIGURE 5·13 BEHAVIOUR OF BELT VELOCITY AND TENSION DURING AN 850 TONS PER HOUR SHUT DOWN WITH MINIMAL BRAKING TORQUE APPLIED AT THE TAIL-END OF B18 CONVEYOR

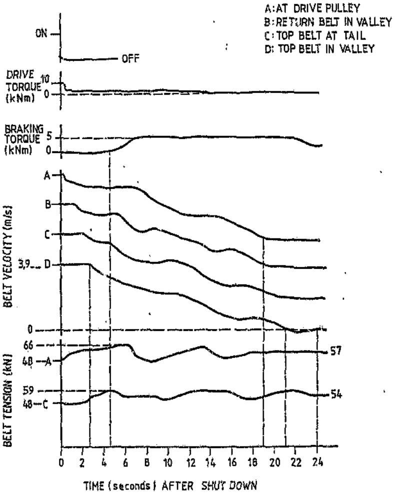

FIGURE 5·13 BEHAVIOUR OF BELT VELOCITY AND TENSION DURING AN 850 TONS PER HOUR SHUT DOWN WITH MINIMAL BRAKING TORQUE APPLIED AT THE TAIL-END OF B18 CONVEYOR

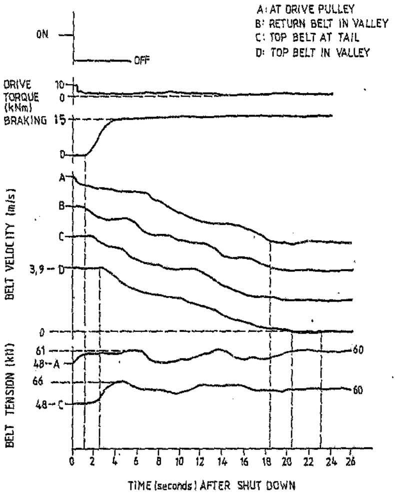

FIGURE 5.14 EFFECT OF HIGH BRAKING TORQUE APPLIED AT THE TAIL-END OF B18 CONVEYOR ON BELT VELOCITY AND BELT TENSION WHILE SHUTTING DOWN THE SYSTEM CARRYING 850 TONS PER HOUR

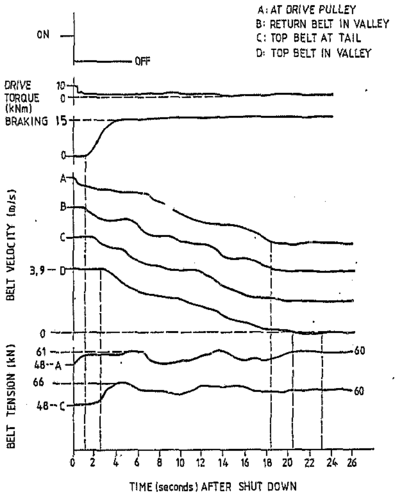

FIGURE 5·14 EFFECT OF HIGH BRAKING TORQUE APPLIED AT THE TAIL-END OF B18 CONVEYOR ON BELT VELOCITY AND BELT TENSION WHILE SHUTTING DOWN THE SYSTEM CARRYING 850 TONS PER HOUR

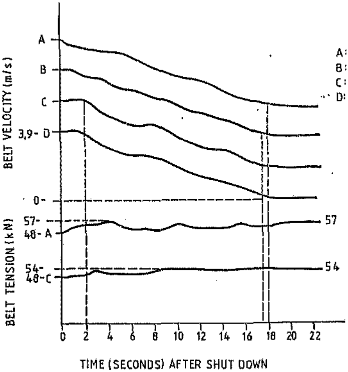

FIGURE 5·16

BELT VELOCITY AND TENSION OF B18 CONVEYOR DURING AN EMPTY SHUT DOWN WITH NO BRAKING TORQUE APPLIED

TACHOMETER LOCATIONS:-

A: AT DRIVE PULLEY
B: RETURN BELT IN VALLEY
C: TOP BELT AT TAIL
D: TOP BELT IN VALLEY

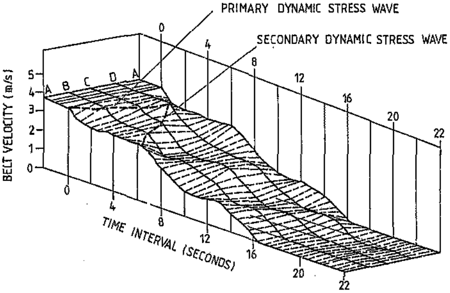

FIGURE 5.18 DYNAMIC STRESS WAVES IN B18 CONVEYOR BELTING DURING AN 850 TONS PER HOUR SHUT DOWN CYCLE.

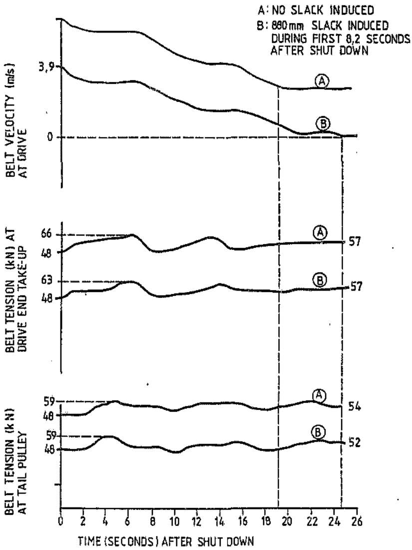

FIGURE 5·20 EFFECT OF INDUCING SLACK INTO THE DRIVE TAKE-UP OF B18 CONVEYOR DURING AN 850 TONS PER HOUR SHUT DOWN CYCLE

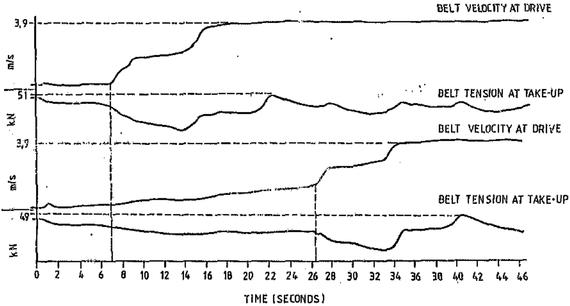

FIG 5·21 START UP TIME DELAY VARIATION FOR A 700 t.p.h. LOAD

TESTS 10 & 23 (21/1)

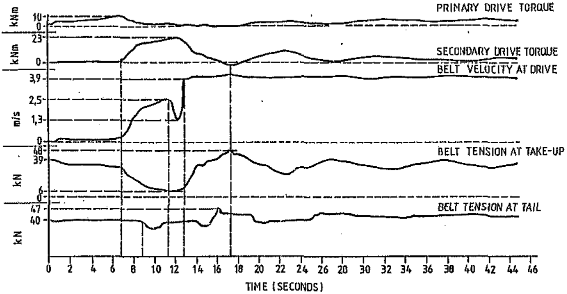

FIG 5·22 EMPTY BELT START-UP WITH 7 SECONDS DELAY BETWEEN PRIMARY & SECONDARY DRIVE MOTORS SWITCHING

TEST 12 (21/1/88)

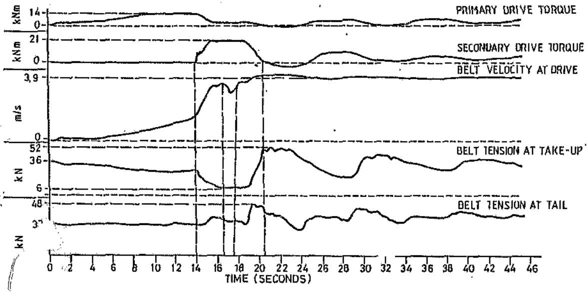

FIG 5·23 EMPTY BELT START-UP WITH 14 SECONDS DELAY BETWEEN PRIMARY & SECONDARY DRIVE MOTORS SWITCHING

TEST 12A (21/1/80)

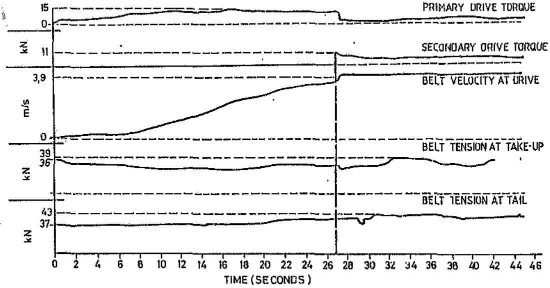

FIG 5·24 EMPTY BELT START UP WITH 27 SECOND DELAY BETWEEN PRIMARY AND SECONDARY DRIVE MOTORS SWITCHING

TEST 12B (21/1/88)

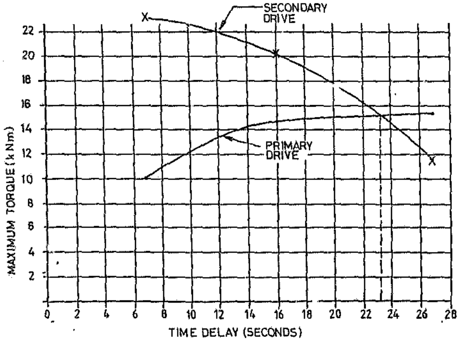

FIG 5·25 MAXIMUM TORQUE VARIATION WITH TIME DELAY BETWEEN PRIMARY AND SECONDARY DRIVES WHEN STARTING B18 CONVEYOR EMPTY

ANNEXURE B

ANGLO AMERICAN CORPORATION OF SOUTH AFRICA LIMITED

MECHANICAL ENGINEERING DEPARTMENT

NOTE FOR THE RECORD

TORQUE MEASUREMENT AND CALIBRATION OF STRAIN ARMS OF 819 CONVEYOR FOR GOEDEHOOP COLLIERY

The calibration procedure of strain gauged drive and brake shafts and the formulas used to derive the torque measured on these shafts is detailed below.

SHEAR STRESS MEASUREMENT

$$\tau = \frac{Tr}{J} \qquad (1)$$

for a solid shaft $J = \pi D^4/32$

$$\tau = \frac{16T}{\pi D^3} \qquad (2)$$

SHEAR STRAIN CONVERSION

$$\gamma = \tau/G = \frac{2\tau(1+v)}{E} \qquad (3)$$

note for pure shear

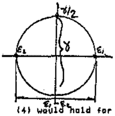

$\epsilon_1 = \epsilon$ (assuming gauge is aligned
$\epsilon_2 = -\epsilon$ along principal axis)

$$\gamma = \epsilon_1 - \epsilon_2 = 2\epsilon \qquad (4)$$

(4) would hold for a two arm active bridge i.e.

$\epsilon_B = 2\epsilon = \gamma$ the bridge strain would be equal to the shear strain

(5)

if a four arm active bridge were used

$$\gamma = \epsilon B/2 \qquad (6)$$

consider (3)

$$\gamma = \tau/G = \frac{2\tau(1+v)}{E}$$

$$\gamma = \frac{32T(1+v)}{E\pi D} \qquad (7)$$

(7) gives the relationship between actual shear strain and torque. The actual *shear strain and bridge* strain are related by the number of gauges which are active. Each gauge is aligned along the principal axis ($\pm$ 45°) and will measure ϵ_1 or ϵ_2.

single active arm: $\epsilon_1 = \epsilon \quad \epsilon_2 = 0 \quad \epsilon B = \epsilon_1 = \epsilon = \gamma/2$ (8)
two active arms : $\epsilon_1 = \epsilon \quad \epsilon_2 = -\epsilon \quad \epsilon B = \epsilon_1 - \epsilon_2 = 2\epsilon = \gamma$ (9)
four active arms : $\epsilon_1 = 2\epsilon \quad \epsilon_2 = -2\epsilon \quad \epsilon B = \epsilon_1 - \epsilon_2 = 4\epsilon = 2\gamma$ (10)
Substituting (8), (9), (10) *into (7)*:

$$\epsilon B^{1} = \frac{16T(1+v)}{E\pi D^3} \qquad \text{single active arm;} \qquad (11)$$

$$\epsilon B^{2} = \frac{32T(1+v)}{E\pi D^3} = 2\epsilon_B^{1} \qquad \text{double active arm} \qquad (12)$$

$$\epsilon B^{4} = \frac{64T(1+v)}{E\pi D^3} = 4\epsilon_B^{1} \qquad \text{four active arms} \qquad (13)$$

<u>CALLIBRATION PROCEDURE</u>

A shunt resistor is placed across one arm of the bridge. This simulates a bridge strain for a single active gauge. However if *in fact more gauges are* active then the calibration strain should be used as a bridge strain and the torque relationship should be calculated according to formuli (11), (12), (13). Alternatively the bridge strain *can be converted* by dividing by the number of active gauges and then calculating the torque relationship as a single active gauge e.g.

calibration signal due to shunt resistance : $\epsilon B = 50\ \mu\epsilon$
four active arms: (13)

$$50 \times 10^{-6} = \frac{64T\ (1+.3)}{200\times 10^{9}\ \pi (0.16)^3} \qquad v = 0,3 \text{ (Poisson's Ratio)} \qquad D = 0{,}16m$$

T = 1546 NM/50 $\mu\epsilon$ 50$\mu\epsilon$B = 375mv (GDHP brake CH1
T = 4122 NM/volt
T = 30,9 NM/$\mu\epsilon$B   (= 2061 NM/CM@500 mv/cm)

Alternatively the method of using the corrected bridge strain could be used.

i.e. a shunt resister equivalent to a 50 $\mu\epsilon$ offset gives an actual bridge strain of 12.5 $\mu\epsilon$.

$$T = 1546\ NM/12.5\ \mu\epsilon\ act = 123.6\ NM/\mu\epsilon\ act$$

Note: The calibration sensitivity Tb, Tact are a factor of four different, however this is due to the factor of 4 between the bridge strain used in Tb and the actual strain used for Tact. Transforming back to units of NM/mv will reveal the same calibration and chart deflections, i.e.

Tact = 123.6 NM/$\mu\epsilon$ act

15 $\mu\epsilon$ act = 450 mv

Tact = 4122 NM/volt (= 2061 NM @ 500 mv/Cm)

As can be seen consistency in the calibration is maintained.

The measured bridge strain used for calibration is calculated according to *the following formula.*

$$\mu\epsilon = \frac{Rg \times 10^6}{GF\ (R + Rg)}$$

$\mu\epsilon$ = measured microstrain
GF = gauge factor
Rg = active gauge resistance
R = shunt gauge resistance

Thus a 966KΩ resistor for a 350Ω bridge (as used for the drive shafts) yields a bridge strain of = 171 $\mu\epsilon$.
Since the gauge factor = 2,12

<u>Note</u> Gauge Resistance for gauges used on the brake shaft is 120Ω with gauge factor 2.1 it is important therefore to always calibrate the strain gauge bridges prior to testing so that the bridge output in terms of mv/$\mu\epsilon$ is known.

In this regard note must be made of these values when analysing the torque traces obtained during tests carried out on the shafts.

<u>Torque measured on drive shafts under an unknown belt load</u>

Strain measurements were taken on 17/12/87 at the drive end of the belt. Reference is made to the attached *traces where the* relationship between the torque, the strain and the analog signal output are made.

A bridge output of 200 mv yields a *bridge microstrain* of 340$\mu\varepsilon$
Applying these *figures in formula* 12 above yields a torque of *14.98kNm for* 200 mv (340 $\mu\varepsilon$) bridge output. The diameter of the shaft is 0.12 m and E is taken as 200x10 N/m

The maximum *starting* torque is then 20,97 KNm for the primary *drive* and 39,7 KNm for secondary drive.

<u>A.VAN DIJK</u>
<u>TEST TECHNICIAN (MECH)</u>
1988.01.14

c.c. Dr.K.A.Wainwright
Mr.H.Dreyer
Mr.C.P.Constancon

AVD/mas/:204/1-8

ANNEXURE
C

ANNEXURE C

THEORETICAL STRESS WAVE VELOCITY CALCULATIONS FOR B18 CONVEYOR

Coulson (1955) derived a formula for the velocity of longitudinal waves in bars and springs.

$$C = \sqrt{\lambda/\rho} \qquad \text{(m/s)} \qquad (1)$$

Where C = longitudinal wave velocity (m/s)
λ = Young's modulus for the material (N/m)
ρ = mass per unit length (kg/m)

Because of the composite construction of conveyor belting, it is customary to refer to the "belt modulus" rather than Young's modulus in conveyor calculations.

Belt modulus E is defined as the allowable belt tension per metre width. As a general rule the suppliers of B18's belting use a figure of

(5,8 x belt class x no. of plies) kN/m for fabric belting.
In the case of B18 conveyor

$$\begin{aligned} E &= 5{,}8 \times 650 \times 3 \text{ kN/m} \\ &= 11310 \text{ kN/m} \\ &= 11310 \times 10^3 \text{ N/m} \end{aligned}$$

It therefore follows that $\lambda = Ew$, where w = belt width (metres)
Equation (1) then becomes.

$$C = \sqrt{Ew/\rho} \qquad \text{(m/s)}$$

Referring to section 5.2.2 in the main project report on B18 conveyor dynamic stress wave behaviour, the following theoretical stress wave velocities were calculated.

Case 1

Stress wave velocity in the carrying strand of B18 conveyor - no load carried

$$V_E = C_1 = \sqrt{EW/\rho_1} \quad m/s$$

where $E = 11310$ kN/m
$W = 1,2$m
$\rho_1 =$ belt mass/m + idler mass/m
$= 13,903 + 15,1$ kg/m
$= 29,003$ kg/m

$$\therefore \quad V_E = \sqrt{11310 \times 10^3 \times 1,2/29,003} \ m/s$$
$$= 684 \ m/s$$

The measured stress wave velocity was 696 m/s

Case 2

Stress wave velocity in the carrying strand of B18 conveyor - 850 tons per hour carried.

In this case ρ is increased by the mass per metre carried:

$= $ Load rate/belt speed
$= 850 \times 1000/(3600 \times 3,9)$ kg/m
$= 60,54$ kg/m
$\therefore \rho_2 = 29,003 + 60,54$ kg/m
$= 89,543$ kg/m

$$\therefore \ V_L = C_2 = \sqrt{11310 \times 10^3 \times 1,2/89,543} \quad m/s$$
$$= 389 \ m/s$$

The measured stress wave velocity was 385 m/s.

Case 3

Stress wave velocity in the return strand of B18 conveyor.

Because of the fewer idlers on the return side of the conveyor, ρ in this case is less than for case 1.

$$\rho_3 = 13{,}903 + 3{,}44 \text{ kg}$$
$$= 17{,}343 \text{ kg/m}$$

$$\therefore V_R = C_3 = \sqrt{11310 \times 10^3 \times 1{,}2/17{,}343} \text{ m/s}$$
$$= 884 \text{ m/s}$$

The measured stress wave velocity was 839 m/s

REFERENCE

Coulson, C A (1955) "Waves, a mathematical account of the common type of wave motion", pp 51-52